Astron. Astrophys. 360, 1157–1162 (2000)

ASTRONOMY AND ASTROPHYSICS

Granular velocities of the Sun from speckle interferometry

J. Krieg, F. Kneer, M. Koschinsky, and C. Ritter

Universitäts-Sternwarte Göttingen, Geismarlandstrasse 11, 37083 Göttingen, Germany

Received 16 February 2000 / Accepted 15 May 2000

Abstract. We present observations of granular velocities and their relation to the granular intensity pattern from the disc center of the Sun. They were obtained in June 1997 with the Vacuum Tower Telescope at the Observatorio del Teide on Tenerife. High spatial resolution, 0.″4–0.″5 for the velocities, was achieved with speckle methods applied to two-dimensional narrow-band images in Na D_2 from the "Göttingen" Fabry-Perot interferometer. The velocity observations refer to a geometric height of 50–200 km (above $\tau_5 = 1$). Velocity amplitudes of $\pm 2.2\,\mathrm{km\,s^{-1}}$ are seen. The high velocity regions are small-scale and the upflows coincide frequently with the bright borders of granules or with small-scale brightenings. A statistical analysis reveals only a rough consistency to the -5/3 or -17/3 law of log(power) vs. log(wavenumber) expected for isotropic turbulence (cf. Espagnet et al. 1993). We consider an agreement with such power laws as accidental since the intensity and velocity power spectra found here decrease smoothly from flat ones at low wavenumbers to steep ones at high wavenumbers. The coherence of velocity and intensity fluctuation stays above 0.5 up to horizontal wavenumbers $k_\mathrm{h} \approx 11\ \mathrm{Mm^{-1}} (\widehat{=} 0.''8)$ and the phase difference between intensity and velocity stays stable down to structures of 0.″5. While the intensity pattern exhibits a clearly non-Gaussian distribution, the velocity distribution can be represented by a Gaussian with a "macroturbulent" velocity of $0.825\,\mathrm{km\,s^{-1}}$.

Key words: Sun: granulation – Sun: photosphere – techniques: image processing – techniques: spectroscopic

1. Introduction

To understand the granular dynamics of the Sun, thus much of the dynamics of late type stars, observations with high spatial resolution are needed. During the last decades, observations have become available from high quality solar telescopes at excellent sites and with sophisticated post-focus instrumentation. A wealth of granular fine structure has become visible. Space allows only to mention few works: Collados et al. (1996) used the Vacuum Tower Telescope (VTT) at the Observatorio del Teide/Tenerife with a correlation tracker in its scanning mode to obtain two-dimensional (2D) spectroscopic information at high spatial and spectral resolution. They could produce maps in narrow wavelength bands to show the intensity and velocity fluctuations at various heights of the photosphere. Likewise, Nesis et al. (1997, 1999, and further references therein) exploited the VTT's high spatial and spectral resolution slit spectrograph to investigate the problem of turbulence generated by granular motions. Espagnet et al. (1993, 1995) obtained high quality data from the multi-channel subtractive double-pass (MSDP) spectrograph at the Pic du Midi solar telescope. They studied the height dependence of intensity and velocity fluctuations from various wavelength positions in the Na D_2 line. A recent review on the solar granulation and its dynamics was presented by Muller (1999) who also references the results from the excellent data obtained with the Swedish solar telescope on San Miguel de la Palma.

The present contribution deals with the continuation of our efforts to reach highest possible spatial resolution from speckle methods combined with 2D spectroscopy by means of a wavelength scanning Fabry-Perot interferometer (FPI) (Krieg et al. 1999, henceforth Paper I). We shall present below an analysis of granular velocities – and their relation to the granular intensity pattern – in a 2D field of view obtained with image restoration techniques.

2. Observations and data analysis

The observations for this work stem from one of the data sets described in Paper I. They were taken on June 21, 1997, with our FPI at the VTT on Tenerife from quiet Sun disc centre. The FPI was scanned through the Na D_2 line with a bandwidth of 200 mÅ at steps of 100 mÅ. At each wavelength position 5 short exposure (6 ms) narrow-band images were taken. Strictly simultaneously with these, integrated light (broad-band) images through a 10 Å interference filter centered at Na D_2 were taken. The image scale on the CCDs (Thompson TH 7863 FT, 384×286 pixels) is 0.″1/pixel leading to an original field of view of 38.″4×28.″6.

A scan over the relevant part of the Na D_2 line takes approximately 18 s. This is not critical for slow convective motions of few $\mathrm{km\,s^{-1}}$. But changes of dynamics occurring on shorter time scales will be smeared out, at least. Modifications of the appa-

Send offprint requests to: F. Kneer (kneer@uni-sw.gwdg.de)

ratus, e.g. by using substantially faster CCDs, to speed up the scanning process are under way.

The *observed* Na D_2 profile is very similar to the fully drawn profile in Fig. 1 of Paper I. As is demonstrated there, the observed profile differs much from one taken with a high resolution spectrograph due to the broad transmission curve of the FPI of 200 mÅ (Airy's formula) and to the transmission curve of the pre-filter needed for order sorting. The line center intensity is increased from 0.04 (relative to the continuum intensity) to 0.31 and the wing intensities are much depressed, while the width of the profile remains approximately unchanged (full width at half minimum = 550 mÅ). We do not treat here the line center region of the profile, and the smearing effect (convolution with Airy's FPI function) is taken into account for the velocity response function (see below). The depression of the wing intensities could be removed from measuring the transmission curve of the pre-filter with a continuous light source (haline lamp). The slopes of the observed profiles are still steep enough to determine shifts for velocity measurements. The results on the velocity analysis are described below.

The data analysis proceeded in the usual way (see also Paper I). We applied dark frame and flat field corrections and shifted the images to correct for image motion. This latter processing reduces the field of view to $32\farcs0 \times 23\farcs4$. Next we reconstructed the *broad-band* images with speckle techniques, i.e. with the spectral ratio method (von der Lühe 1984) and with speckle masking (Weigelt 1977). The *narrow-band* reconstructions were also obtained as in Paper I, by means of the instantaneous optical transfer functions derived from a combination of the simultaneous broad-band images and the broad-band speckle reconstruction.

Here, for the determination of the granular velocities in the low photosphere, we combined the images at -500 mÅ and -600 mÅ off line center, and at +500 mÅ and +600 mÅ giving 10 images for reconstruction in the blue and red wing of Na D_2, respectively. The Doppler shifts are measured from the differences of the intensity fluctuations in the blue and red wing via

$$\Delta I_{\rm blue} - \Delta I_{\rm red} = \left(\frac{dI}{d\lambda}\bigg|_{\rm blue} - \frac{dI}{d\lambda}\bigg|_{\rm red} \right) \Delta\lambda \,. \qquad (1)$$

The $dI/d\lambda$ values are taken from the average D_2 profile *observed* with the FPI. To build the difference of the intensity fluctuations in the above equation identical optimum noise filters (Brault & White 1971) were applied to the blue and red wing intensity fluctuations. This is done by using the product of the noise filters obtained from the data of both wings (and the flat fields). From the wavenumber cutoffs of the noise filters we estimate a spatial resolution of our velocity measurements of $0\farcs4$–$0\farcs5$. The speckle reconstruction of the granular intensities has a better spatial resolution, approximately $0\farcs2$.

The height of formation of the velocity signal is best seen from response functions (Mein 1971, Kneer & Nolte 1994, cf. also Paper I). Following the prescription by Mein (1971) and according to Eq. (1), it is obtained from the intensity changes due to a velocity pulse at a limited height range $[z, z + \Delta z]$. We show in Fig. 1 the (normalized) velocity response function

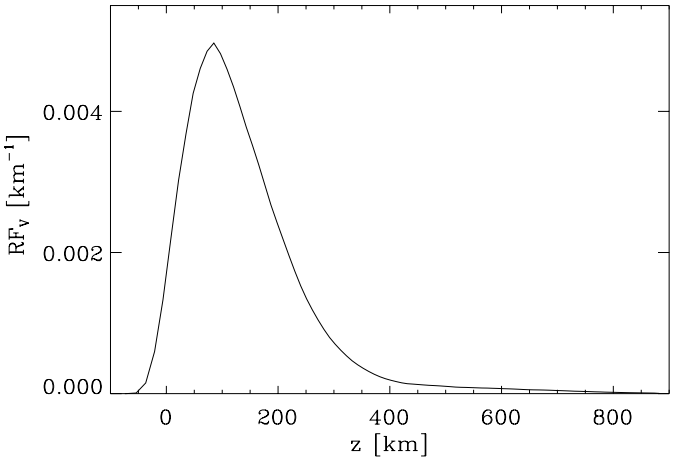

Fig. 1. Velocity response function for the measurements in the band 500–600 mÅ off the center of Na D_2. The instrumental profile of the FPI spectrometer is taken into account. The calculation was performed in LTE with the model of Vernazza et al. (1981).

$RF_{\rm v}(z)$ calculated in LTE for the $\Delta\lambda$ = 500–600 mÅ off D_2 line center velocity measurements. Here, the limited spectral resolution is accounted for. The center of gravity of $RF_{\rm v}$ in Fig. 1 is at $\bar{z}$ = 140 km (above τ_5 = 1).

3. Results and discussion

3.1. Intensity and velocity maps

Fig. 2 gives in its upper part the speckle-reconstructed integrated white light (broad-band) image of the granulation in the quiet Sun. The intensity fluctuations have a contrast of $\Delta I_{rms}/\bar{I} = 0.087$. This contrast value is low compared to those of reconstructed granular images described elsewhere (cf. references in Muller 1999) due to differences in the characteristics of the used spectral line.

The lower part of Fig. 2 shows the velocity map. Here, to reduce the influence of the 5-min oscillations on the velocity we present the residual values after smoothing over $3\farcs5 \times 3\farcs5$. The velocities range from -2.10 km s^{-1} (downflows) to +2.34 km s^{-1} (upflows) in the low photosphere. This is about a factor of 3 larger than those presented by Nesis et al. (1999) from excellent spectrograms taken with a slit spectrograph. Without smoothing, the velocity exhibits a *rms* value of $v_{\rm rms}$ = 0.625 km s^{-1}. The smoothing reduces this only a little to $v_{\rm rms}$ = 0.575 km s^{-1}, which is somewhat larger than the value obtained by Deubner (1988) from likewise excellent spectra from the VTT at Sacramento Peak Observatory. But it is substantially below the value of $v_{\rm rms}$ = 1.5 km s^{-1} given by Espagnet et al. (1995) for the low photosphere from their MSDP data, which are uncorrected for seeing. Even for the middle and upper photosphere, the latter authors give larger *rms* values than we find here. Espagnet et al. (1995) demonstrate that most of the *rms* velocities are due to motions at scales $> 1\farcs4$. However, all the way during data processing we took care to avoid leakage of the power as much as possible and do trust our reconstructed

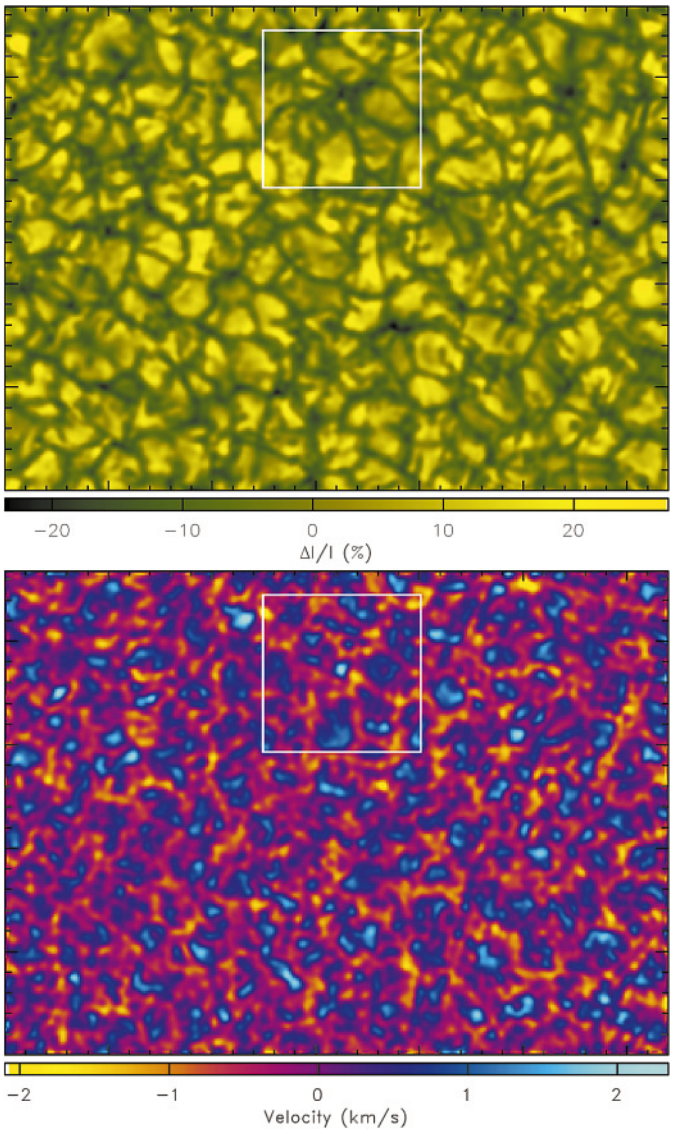

Fig. 2. Granular intensity and velocity at quiet Sun disc center. The velocity map shows the residuals after boxcar smoothing over 3.″5×3.″5. Tickmarks are at 1″ distance.

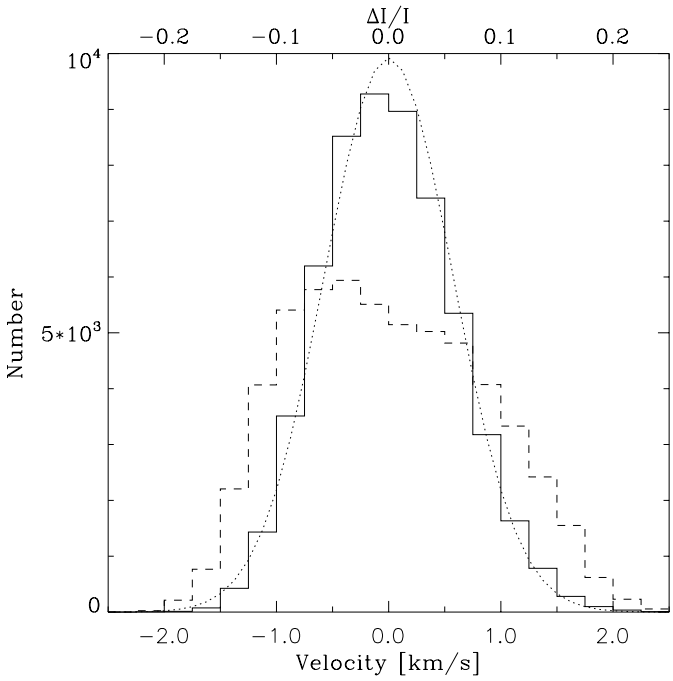

Fig. 3. Histograms of velocity (solid, lower abscissa) and intensity (dashed, upper abscissa). The dotted curve is a Gaussian with a "macro-turbulent" velocity of $V = 0.813\,\mathrm{km\,s^{-1}}$.

small band image at least down to 0.″5. Thus the reason for this discrepancy remains to be clarified.

High velocities occur only rarely and we do not see extreme downdrafts in intergranular lanes as expected for the *low photosphere* from numerical simulations (Nordlund et al. 1997). Instead, we see approximately the same number of fast upward flows as downward flows. Fast upward flows may occur in small structures. For instance, in the middle of the white box of Fig. 2, we see a small-scale bright point in the intensity image at the spatial resolution limit. The upward velocity coinciding with this structure amounts to about $2\,\mathrm{km\,s^{-1}}$. Close by, 0.″6 towards the right, the downflow in the intergranular space is $-2\,\mathrm{km\,s^{-1}}$. Further close inspection of Fig. 2 shows that many of the other fast upflow velocities coincide with the bright borders of granules (de Boer et al. 1992, Rast 1995 and Wilken et al. 1997). One example is clearly seen in the large granule just below the above mentioned bright point. This supports the identification of the cause of the bright granular rims as upcoming hot material at locations of reduced pressure, as suggested from numerical simulations by Steffen et al. (1994).

A word on the elimination of the signal of the 5-min oscillations is appropriate. Deubner (1988), Espagnet et al. (1995) and Hirzberger (1998) demonstrated how to properly disentangle oscillations in the 5-min period range and at shorter periods from granular flows, via filtering in the $k-\omega$ plane. Yet here, we do not deal with a time sequence and thus only a filtering in space is possible. According to Espagnet et al. (1996) the 5-min oscillations occur at wavelengths $\geq 4''$–$8''$(see e.g. Fig. 8 in Espagnet et al. 1996). Thus, since we are interested in the very small scale dynamics, the influence of the 5-min oscillations after only spatial smoothing should be low, although shorter period waves at small scales may destroy the granular intensity - velocity correlations (see Espagnet et al. 1995 and the discussion below). In any case, time sequences are certainly needed in the future.

3.2. Statistical analysis

Fig. 3 gives histograms of the residuals of the 3.″5×3.″5 smoothed velocities (solid) and of the residuals of the likewise smoothed intensity fluctuations (dashed). The intensities are far from exhibiting a normal distribution, the granular intensity pattern is non-Gaussian. Although Fig. 2 shows also a clear distinction between isolated upflow regions and contiguous regions of downflows, the velocity histogram possesses only a small skewness. Apart from this it is well fitted by a Gaussian distribution

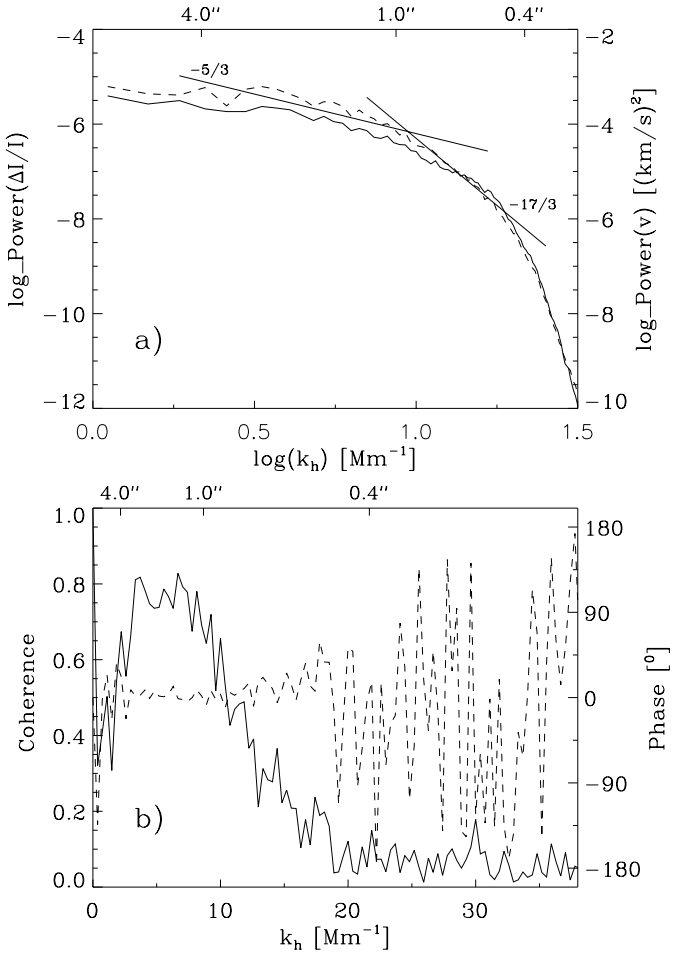

Fig. 4. a Power spectra of velocity (solid) and intensity (dashed) fluctuations on a *log-log* scale. For the straight lines ($-5/3$ and $-5/17$) see the text. **b** Coherence (solid) and phase difference (dashed) between intensity and velocity.

$N(v) \sim \exp[-(v/V)^2]$ with $V = 0.813\,\mathrm{km\,s^{-1}} = \sqrt{2}v_{\mathrm{rms}}$ and $v_{\mathrm{rms}} = 0.575\,\mathrm{km\,s^{-1}}$ from above (dotted curve in Fig. 3). As already mentioned, we do not see, at heights of 50–200 km, fast downdrafts at intergranular regions expected from numerical simulations for the *deep photosphere* (Nordlund et al. 1997). The reason for this "non-detection" may be found from simulations of the granular convective dynamics by Solanki et al. (1996, Fig. 1 there) and Gadun et al. (1999, Fig. 2.). There it is seen that the difference between the mild, broad upflows and the strong, narrow downflows in deep layers is dissolved at larger heights where downward flows have become broader and cover a larger area.

Power, coherence, and phase spectra of the white light image are depicted in Fig. 4a and b. They are azimuthal averages in the (horizontal) $k_{\mathrm{x}} - k_{\mathrm{y}}$ plane, from the non-smoothed data, giving high statistical significance. The straight lines in the *log-log* representations of the power spectra (Fig. 4a)) indicate the exponential decays for an inertial convective range ($-5/3$) and an inertial conductive range ($-17/3$) in isotropic turbulence (cf. Espagnet et al. 1993 and Muller 1999). The vertical positions of the straight lines were chosen freely to come close to the power spectra measured here. While the overall agreement to these theoretical slopes is not too bad, the smooth decrease of the power spectra in Fig. 4a does not necessarily suggest such kind of turbulence and looks different to the results of Muller (1999). Also, a distinct change of the slope near 1.″4, as in Espagnet et al. (1993) does not appear in our high spatial resolution data. If at all, a change of slope may occur for the velocity power spectrum at structural wavelengths of about 0.″9. Nordlund et al. (1997), from considerations of fluid dynamics and from numerical simulations, have presented reasons that granular convection of the stratified solar gas should be essentially laminar and not compatible with isotropic turbulence. The sharp decline of the power below 0.″4 is due to our optimum filter and does not reveal any physical relevance.

In Fig. 4b the coherence between velocity and intensity fluctuations drops below 0.5 at horizontal wavenumbers $k_{\mathrm{h}} = 11$ $\mathrm{Mm^{-1}}$ ($\widehat{=}$ 0.″8). Thus the coherence between the granular intensity pattern and the flow stays high to much smaller structures than observed hitherto, e.g. with the MSDP by Espagnet et al. (1995) or from excellent slit spectrograms by Deubner (1988). The coherence of motions with intensity at small scales is also much higher than in the data presented earlier by Wiehr & Kneer (1988) also from one-dimensional spectrograms. Likewise, the phase difference stays stable at 0° up to $k_{\mathrm{h}} \approx 17.5\,\mathrm{Mm^{-1}}$. This corresponds to 0.″5, which is approximately the estimated spatial resolution of the velocity map. We agree with Deubner's (1988) notion that the loss of coherence may be caused by a change of character of the flow due to the appearance of internal gravity waves. Yet, if so, our observations show that this occurs at substantially smaller scales than 0.″95–1.″25 proposed by Deubner.

Turbulence in a gravitationally stratified atmosphere is in itself an interesting phenomenon. Even if it is difficult to see directly turbulence on the Sun from velocity measurements, at least with the limitations posed by the spatial resolution of today's telescopes, we may still ask under which conditions and where turbulent flows occur.

Thus, finally, we search for large velocity differences at short spatial distances. The places where these occur are the most likely regions where turbulence and short period waves are generated (see e.g. Nesis et al. 1997, 1999, for discussions of turbulence and Musielak et al. 1994, for wave generation). From the reasoning by Nordlund et al. (1997) it is suggested that the regions of intergranular downflows are the best candidates for turbulence generation due to strong velocity gradients. Therefore, we start with the downflows and divide the field of view into squares of 0.″7×0.″7 and simply locate in each square the *minimum* velocity, omitting the according positions if the velocity at any pixel next to the square border is still smaller. We then ask for the number of occurrences of velocity differences, in steps of $0.5\,\mathrm{km\,s^{-1}}$, in circular areas of 0.″5 and 1.″0 radius about the minimum positions. Still larger scales are easy to implement but of little interest since we search for large velocity changes on short distances. Fig. 5 gives the corresponding histograms. It is seen that large differences up to 4–5 $\mathrm{km\,s^{-1}}$ do

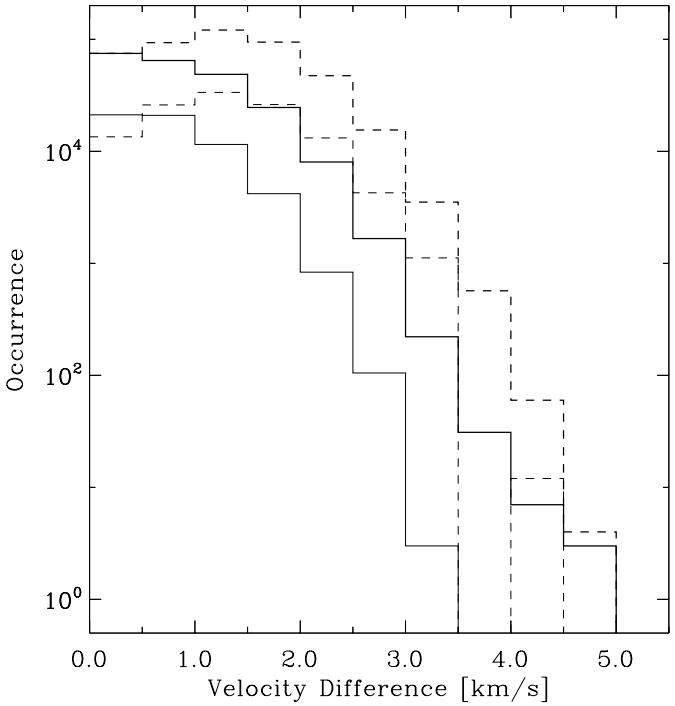

Fig. 5. Occurrences of velocity differences between velocity minima in squares of $0\farcs7\times0\farcs7$ and ambient velocities in circles of $1\farcs0$ radius (solid-thick) and $0\farcs5$ radius (solid-thin) centered at the minimum position. The dashed-thick and dashed-thin distributions are the occurrences after reshuffling randomly the positions within the field of view of the velocity data for circles of $1\farcs0$ radius and $0\farcs5$ radius, respectively. (See the text).

occur, but only rarely, only 10 times for the search within the $1\farcs0$ radius circles. They are a very intermittent phenomenon in the $32\farcs0\times23\farcs4$ field of view. Smaller differences of 2–3 km s^{-1} are seen more often, 930 times within the small $0\farcs5$ circle search, or about 1.25 times per $1''\times1''$.

We show also in Fig. 5 the occurrence of velocity differences after *randomly reshuffling* the positions of the velocities, for the same circles ($0\farcs5$ and $1\farcs0$). This is a test on how much the occurrence is influenced by the data and by the method. The differences vs. the result with the original flow pattern are seen to be large. Randomly reshuffled positions of the velocities, but otherwise with the identical distribution as in Fig. 3 (solid curve) result in an order of magnitude larger numbers of occurrence in the middle range of velocity differences than the original data. The distribution of velocity differences is thus an intrinsic property of the granular flow.

The relevance of such velocity gradients must be further investigated in comparison with numerical simulations. And it will certainly be interesting and important to observe with still higher spatial resolution, that is with a telescope with larger aperture than that of the VTT.

If we search for velocity differences from the maximum velocities, the histograms look very similar, which is not obvious *a priori*. The reasons are very likely the same as given above for the nearly Gaussion velocity distribution: Numerical simulations show that at layers of 50–200 km both up- and downflows occur more equally distributed than at the bottom of the photosphere.

4. Conclusion

We have shown above (and in Paper I) that high spatial resolution spectroscopy is possible by combining speckle reconstruction with two-dimensional narrow-band imaging. This allows to study the dynamics of the fine structure of the solar atmosphere. High granular velocities and velocity differences are seen at small scales. A turbulent decay of the granulation, either of intensity or of velocity, i.e. a decrease of log(power) vs. log(wavenumber) with $-5/3$ or $-17/3$ could only roughly be confirmed from our high spatial resolution data. Coherence and phase difference of intensity and velocity fluctuations indicate convective motions down to scales of $0\farcs5$.

The results are encouraging and further investigations with the same or with better resolution are to follow. The analysis of time sequences will allow the proper separation of granular motions from evanescent (5-min period) and short period waves. This will give insight into the temporal evolution of both granular dynamics and waves at small structural lengths. Smaller bandwidths in wavelength than used here will lead to a better discrimination of the height ranges from which the signals stem. And finally, studies of structures with sizes smaller than $0\farcs2$–$0\farcs4$ need more photons from telescopes with larger aperture than the VTT on Tenerife.

Acknowledgements. We thank Dr. J. Hirzberger for helpful criticism. The comments of the unknown referee helped to improve substantially the presentation of this work. Financial support by the *Deutsche Forschungsgemeinschaft* through grants KN 152/17-1,2 and KN 152/19-1,2 and by the *Graduiertenkolleg* "Strömungsinstabilitäten und Turbulenz" is gratefully acknowledged. The Vacuum Tower Telescope at the Spanish Observatorio del Teide of the Instituto de Astrofísica de Canarias/Tenerife is operated by the Kiepenheuer-Institut für Sonnenphysik in Freiburg, Germany.

References

Brault J.W., White R.O., 1971, A&A 13, 169
Collados M., Rodríguez Hidalgo I., Ballesteros E., et al., 1996, A&AS 115, 367
de Boer C.R., Kneer F., Nesis A., 1992, A&A 257, L4
Deubner F.-L., 1988, A&A 204, 301
Espagnet O., Muller R., Roudier Th., Mein N., 1993, A&A 271, 589
Espagnet O., Muller R., Roudier Th., Mein N., Mein P., 1995, A&AS 109, 79
Espagnet O., Muller R., Roudier Th., et al., 1996, A&A 313, 297
Gadun A.S., Solanki S.K., Johannesson A., 1999, A&A 350, 1018
Hirzberger J., 1998, PhD thesis, University of Graz
Kneer F., Nolte U., 1994, A&A 286, 309
Krieg J., Wunnenberg M., Kneer F., Koschinsky M., Ritter C., 1999, A&A 343, 983 (Paper I)
Mein P., 1971, Solar Phys. 20, 3
Muller R., 1999, The solar granulation, in: Hanslmeier A., Messerotti M. (eds.), Motions in the Solar Atmosphere, Astrophysics and Space Science Library. Dordrecht: Kluwer, p. 5

Musielak Z.E., Rosner R., Stein R.F., Ulmschneider P., 1994, ApJ 423, 474
Nesis A., Hammer R., Hanslmeier A., et al., 1997, A&A 326, 851
Nesis A., Hammer R., Kiefer M., et al., 1999, A&A 345, 265
Nordlund Å, Spruit H.C., Ludwig H.-G., Trampedach R., 1997, A&A 328, 229
Rast M.P., 1995, ApJ 443, 863
Solanki S.K., Rüedi I., Bianda M., Steffen M., 1996, A&A 308, 623
Steffen M., Freytag B., Holweger H., 1994, Shocks in the solar photosphere and their spectroscopic signature, in: Schüssler M., Schmidt W. (eds.), Solar Magnetic Fields. Cambridge: Univ. Press, p. 298
Vernazza J.E., Avrett E.H., Loeser R., 1981, ApJS 45, 635
von der Lühe O., 1984, J. Opt. Soc. Am. A1, 510
Weigelt G.P., 1977, Optics Comm. 21, 55
Wiehr E., Kneer F., 1988, A&A 195, 310
Wilken V., de Boer C.R., Denker C., Kneer F., 1997, A&A 325, 819